Wave-induced mixing in the upper ocean: Distribution and application to a global ocean circulation model

Fangli Qiao,[1] Yeli Yuan,[1] Yongzeng Yang,[1] Quanan Zheng,[2] Changshui Xia,[1] and Jian Ma[1]

Received 25 February 2004; revised 22 April 2004; accepted 3 May 2004; published 3 June 2004.

[1] From the Reynolds stress expression, the wave-induced vertical viscosity (or diffusivity) *Bv* is defined, which can be used as a parameter to estimate the strength of wave-induced mixing. In addition, a parameter D_5 is introduced to represent a wave-induced mixing penetration depth. The global distribution of *Bv* averaged over the upper 20 m is calculated and its latitudinal transects in boreal summer and winter is discussed. The results show that in summer the wave-induced mixing is strong in the southern oceans south of 30°S, and in winter it is strong in the north Pacific and the north Atlantic north of 30°N, as well as in the southern oceans south of 40°S. Adding *Bv* to the vertical diffusivity in a global ocean circulation model yields a temperature structure in the upper 100 m that is closer to the observed climatology than a model without the wave-induced mixing. *INDEX TERMS:* 4560 Oceanography: Physical: Surface waves and tides (1255); 4568 Oceanography: Physical: Turbulence, diffusion, and mixing processes; 4572 Oceanography: Physical: Upper ocean processes. **Citation:** Qiao, F., Y. Yuan, Y. Yang, Q. Zheng, C. Xia, and J. Ma (2004), Wave-induced mixing in the upper ocean: Distribution and application to a global ocean circulation model, *Geophys. Res. Lett.*, *31*, L11303, doi:10.1029/2004GL019824.

1. Introduction

[2] Overestimated sea surface temperature (SST) and underestimated mixed layer (ML) depth in summer are common problems of ocean circulation models [*Martin*, 1985; *Kantha and Clayson*, 1994]. It is believed that the two problems are caused by insufficient surface mixing. *Ezer* [2000] simulated ML more realistically by including shortwave radiation penetration together with improving parameterization of dissipation in the Mellor-Yamada scheme [*Mellor and Yamada*, 1982]. *Craig and Banner* [1994] and *Mellor* [2003] suggested that surface waves can enhance mixing in the upper ocean. However, parameterization of wave-induced mixing for three-dimensional models remains a challenge. Based on the wave-current coupled model suggested by *Yuan et al.* [1999], we developed the MASNUM (Marine Science and Numerical Modeling) wave-current coupled model and postulated a wave-induced mixing term *Bv* as a function of wave number spectrum. This work gives the spatial and temporal distributions of *Bv* using the MASNUM wave number spectral model [*Yuan et al.*, 1991] and introduces it to an ocean model.

2. Methodology

[3] The current velocity, temperature and salinity can be decomposed into two components, a mean and a fluctuation,

$$U_i = \overline{U_i} + u_i, \quad T = \overline{T} + \theta, \quad S = \overline{S} + s, \tag{1}$$

where $\overline{U_i}$, $\overline{T}$, $\overline{S}$ and u_i, θ, s represent the means and fluctuations of the velocity, temperature, and salinity, respectively, and subscripts i = 1, 2, 3 represent axes of the Cartesian coordinates (x, y, z). The velocity fluctuation can further be decomposed into a turbulence portion u_{ic} and a wave-induced fluctuation u_{iw} , i.e.,

$$u_i = u_{iw} + u_{ic}. \tag{2}$$

Thus, the Reynolds stress can be written as

$$-\overline{u_i u_j} = -\overline{u_{iw} u_{jw}} - \overline{u_{iw} u_{jc}} - \overline{u_{ic} u_{jw}} - \overline{u_{ic} u_{jc}}, \tag{3}$$

where the first term on the right-hand side is the wave-induced Reynolds stress. The fourth term is the turbulence viscosity which could follow the Mellor-Yamada scheme or Prandtl theory [*Fang and Ichiye*, 1983]. Similarly, the Reynolds diffusivity of temperature and salinity can be written as,

$$-\overline{u_i \theta} = -\overline{u_{iw} \theta} - \overline{u_{ic} \theta}, \tag{4}$$

$$-\overline{u_i s} = -\overline{u_{iw} s} - \overline{u_{ic} s}, \tag{5}$$

where the second terms on the right-hand side represent the turbulence diffusivity.

[4] From a linear theory of ocean waves [*Yuan et al.*, 1999], on the wave number spectrum level, the wave-induced fluctuation can be expressed as,

$$u_{iw} = \begin{cases} \iint\limits_{\vec{k}} \omega \frac{k_x}{k} A(\vec{k}) \exp(kz) \exp\left[i(\vec{k} \cdot \vec{x} - \omega t)\right] d\vec{k} \\ \iint\limits_{\vec{k}} \omega \frac{k_y}{k} A(\vec{k}) \exp(kz) \exp\left[i(\vec{k} \cdot \vec{x} - \omega t)\right] d\vec{k} \\ \iint\limits_{\vec{k}} -i\omega A(\vec{k}) \exp(kz) \exp\left[i(\vec{k} \cdot \vec{x} - \omega t)\right] d\vec{k} \end{cases} \tag{6}$$

[1]The First Institute of Oceanography, State Oceanic Administration, Qingdao, China.
[2]Department of Meteorology, University of Maryland, College Park, Maryland, USA.

0094-8276/04/2004GL019824

where $A(\vec{k})$ represents the wave amplitude, ω is the wave angular frequency, k is the wave number, and z is the vertical coordinate axis downward positive with $z = 0$ at the surface.

[5] It is believed that the vertical scales of the wave-induced turbulence and the current turbulence following the Mellor-Yamada scheme are comparative [*Ezer*, 2000]. Based on Prandtl theory and equation (6), the second and third terms of equation (3) and the first terms of equations (4) and (5) representing the wave-induced mixing can be derived as

$$-\left(\overline{u_{iw}u_{jc}} + \overline{u_{ic}u_{jw}}\right) = \begin{pmatrix} 0 & 0 & B_V \dfrac{\partial \overline{U_1}}{\partial z} \\ 0 & 0 & B_V \dfrac{\partial \overline{U_2}}{\partial z} \\ B_V \dfrac{\partial \overline{U_1}}{\partial z} & B_V \dfrac{\partial \overline{U_2}}{\partial z} & 2B_V \dfrac{\partial \overline{U_3}}{\partial z} \end{pmatrix}, \quad (7)$$

$$\left(-\overline{u_{iw}\theta}, -\overline{u_{iw}s}\right) = \begin{pmatrix} 0 & 0 \\ 0 & 0 \\ B_V \dfrac{\partial \overline{T}}{\partial z} & B_V \dfrac{\partial \overline{S}}{\partial z} \end{pmatrix}. \quad (8)$$

Parameter Bv is defined as the wave-induced vertical kinematic viscosity (or diffusivity),

$$B_V = \overline{l_{3w}u'_{3w}}, \quad (9)$$

where the mixing length of the wave-induced turbulence, $l_{3,w}$, is proportional to the range of the wave particle displacement,

$$l_{3w} \sim \iint_{\vec{k}} A(\vec{k}) \exp(kz) \exp\left[i\left(\vec{k} \cdot \vec{x} - \omega t\right)\right] d\vec{k} \quad (10)$$

and u'_{3w} is the increment of vertical wave velocity, u_{3w}, at the mixing length of l_{3w}, which can be expressed as,

$$u'_{3w} = l_{3w} \frac{\partial}{\partial z} \left[\iint_{\vec{k}} \omega^2 E(\vec{k}) \exp(2kz) d\vec{k} \right]^{\frac{1}{2}}, \quad (11)$$

where $E(\vec{k})$ represents the wave number spectrum which contains wind wave and swell.

[6] From equations (9) and (11),

$$B_V = \overline{l_{3w}^2} \frac{\partial}{\partial z} \left[\iint_{\vec{k}} \omega^2 E(\vec{k}) \exp(2kz) d\vec{k} \right]^{\frac{1}{2}}, \quad (12)$$

And from equation (10),

$$\overline{l_{3w}^2} = \alpha \iint_{\vec{k}} E(\vec{k}) \exp(2kz) d\vec{k}, \quad (13)$$

where coefficient $\alpha = O(1)$ should be calibrated by observations.

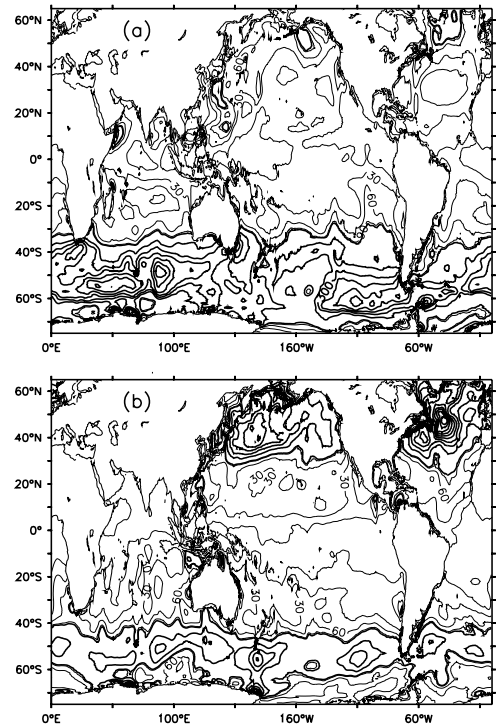

Figure 1. The spatial distributions of the monthly mean upper 20 m averaged Bv (a) in August, and (b) in February. Contour interval is 30 cm^2 s^{-1} from 0 to 90 cm^2 s^{-1} (light line), and 100 cm^2 s^{-1} from 100 to 1000 cm^2 s^{-1} (dark line).

[7] Thus, the expression of Bv is developed as follows,

$$B_V = \alpha \iint_{\vec{k}} E(\vec{k}) \exp(2kz) d\vec{k} \frac{\partial}{\partial z} \cdot \left[\iint_{\vec{k}} \omega^2 E(\vec{k}) \exp(2kz) d\vec{k} \right]^{\frac{1}{2}}. \quad (14)$$

[8] From equations (7) and (8), one can see that Bv is a key factor for determining the wave-induced mixing strength and should be added to ocean circulation model as a part of the vertical kinematic viscosity (or diffusivity).

3. Results

3.1. Global Distribution of Wave-Induced Mixing

[9] In this study the MASNUM wave number spectrum is used to compute Bv with $\alpha = 1$. The computational domain is 75°S–65°N, 0–360°E with a horizontal resolution of 0.5° by 0.5°. The NCEP (National Center for Environmental Prediction) reanalyzed wind fields with the horizontal resolution of 1.25° by 1.0° and time interval of 6 hours interpolated into the model grid are used to calculate the wave number spectrum. Figure 1 shows the distribution of Bv averaged over the upper 20 m in August (Figure 1a) and in February (Figure 1b). One can see that in summer, high values of Bv related to a large surface wave height (not shown) are distributed in the southern oceans. The maximum reaches 600 cm^2 s^{-1} in the southern Indian Ocean. In winter, high values appear in the North Pacific, North

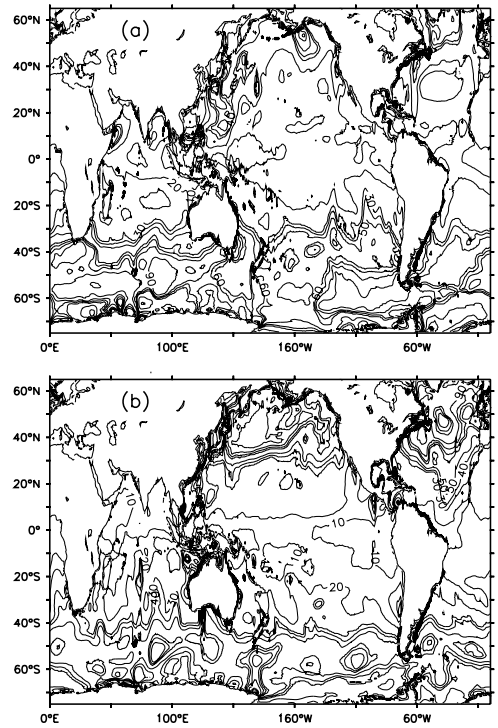

Figure 2. The global distribution of the monthly mean D_5 (a) in August, and (b) in February. Contour interval is 10 m.

Atlantic, and the southern oceans. The maximum reaches 800 $cm^2\ s^{-1}$ in the North Atlantic.

[10] Recent studies on deep ocean mixing indicate that 2–4 $cm^2\ s^{-1}$ are a threshold for a mixing process to play a role in vertical water mass transport [*Ledwell et al.*, 2000; *Polzin et al.*, 1997]. Therefore, we define a wave-induced mixing penetration depth D_5 is the depth at which *Bv* decreases to 5 $cm^2\ s^{-1}$. The physical meaning of D_5 is a characteristic depth of wave-induced mixing. The global distribution of D_5 is shown in Figures 2a (August) and 2b (February). It is readily seen that in boreal summer, the wave-induced mixing can penetrate deep ($D_5 > 50$ m) in the southern oceans, where the maximum value reaches 90 m. In other parts of the world oceans, D_5 is within the range from 10 to 30 m. In boreal winter, deep penetrating wave-induced mixing (D_5 larger than 50 m) appear in the area south of 40°S in the southern oceans, north of 30°N in the Pacific, north of 15°N in the Atlantic with the maximum values of 120 m in the North Atlantic, 90 m in the North Pacific and the southern oceans. This implies that wave-induced mixing in the North Atlantic is much stronger than that in the North Pacific and the Southern Oceans.

3.2. Latitudinal Transects

[11] To show basin-scale variability of the wave-induced mixing, latitudinal transects of *Bv* along the dateline in the Pacific are computed. Figure 3 represents the significant surface wave height and the related vertical structure of wave-induced mixing in the Pacific in boreal summer. One can see that the *Bv* contours are asymmetric with respect to the equator. The high values (>300 $cm^2\ s^{-1}$) are distributed between 40°S and 70°S where D_5 reaches 60 m. At other latitudes, D_5 is shallower than 30 m. Figure 4 represents a case of boreal winter. The *Bv* structure in winter is more

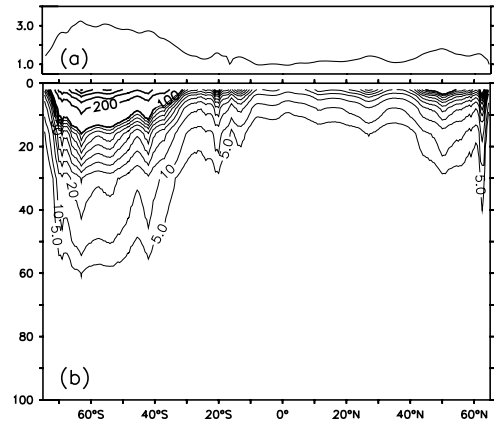

Figure 3. (a) The monthly mean significant surface wave height along the dateline in the Pacific in August (Units are in m). (b) A latitudinal transect of the related *Bv*. Contour interval is 10 $cm^2\ s^{-1}$ from 0 to 100 $cm^2\ s^{-1}$ (light line), and 100 $cm^2\ s^{-1}$ from 100 to 1400 $cm^2\ s^{-1}$ (dark line).

symmetric with respect to the equator than in summer. There are two regions of high value, one located between 50°S and 70°S (D_5 reaches 83 m at 55°S), and the other between 40°N and 65°N (D_5 reaches 100 m at 55°N).

4. Application to a Global Ocean Circulation Model

[12] To evaluate the effects of the wave-induced mixing in the upper ocean, Princeton Ocean Model [*Blumberg and Mellor*, 1987] is run with an enhanced vertical mixing,

$$Km = Km_C + Bv, Kh = Kh_C + Bv, \tag{15}$$

where *Km* and *Kh* are the vertical viscosity and diffusivity used in the model, respectively, Km_C and Kh_C represent the turbulence mixing following the Mellor-Yamada scheme, and *Bv* is an additional term due to waves discussed in this study. The model domain is 75°S–65°N, 0–360°E with a horizontal resolution of 0.5° by 0.5° and 16 vertical sigma layers. The topography is from ETOPO5 and the maximal water depth is chosen as 3000 m, so that at least 5 layers are in the top 100 m. The wind stress and surface heat flux are

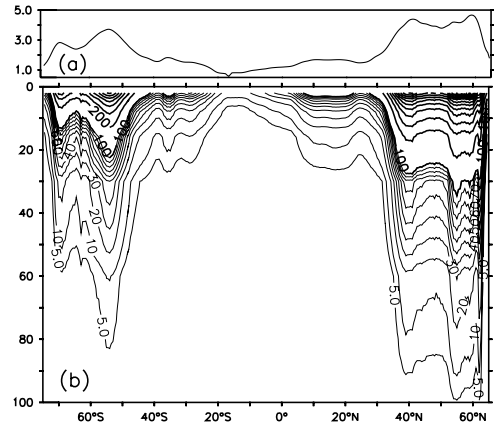

Figure 4. Same as Figure 3, but in February.

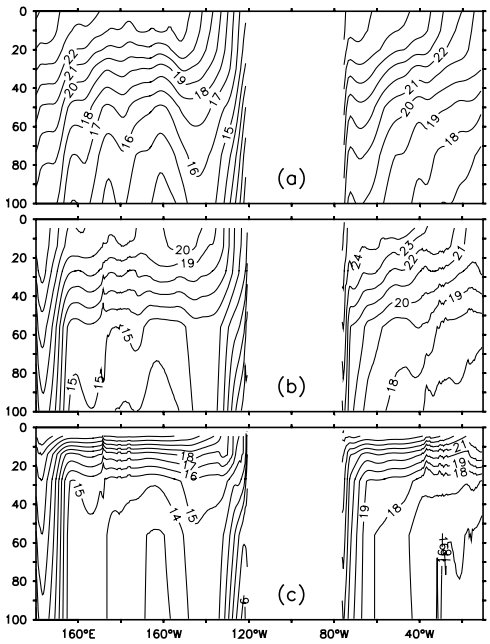

Figure 5. The monthly mean temperature distributions (a) from Levitus data, (b) simulated with wave-induced mixing, and (c) without wave-induced mixing in the Pacific and Atlantic along 35°N in July. Contour interval is 1°C.

taken from the monthly climatological data of the Comprehensive Ocean-Atmosphere Data Set (COADS) with the resolution of 1° by 1°. The model ocean is initially at rest with temperature and salinity taken from the *Levitus* [1982] dataset. Since only the upper ocean is considered, two cases have been run for 6 years and the results, with or without wave-induced mixing, are compared. The simulated temperature structures of the upper 100 m Pacific and Atlantic along 35°N in July are quite different. Result obtained from a model coupled with wave-induced mixing produced temperature distribution (Figure 5b) that is much closer to the Levitus data (Figure 5a), as compared with results obtained from a model without wave-induced mixing (Figure 5c). Similar results were also obtained in other zonal or meridional transects and SST distribution (not shown). Our results, thus, indicate that the wave-induced mixing may play an important role in the regulation of the temperature distribution in the upper 100 m.

[13] But comparing Figures 5a and 5b, one can still find some differences. That means there is still some room left for further study, including the calibration of coefficient α and other mechanisms to improve upper ocean mixing, such as wave breaking.

5. Summary

[14] The wave-induced vertical kinematic viscosity (or diffusivity) parameter *Bv* is derived and used to estimate the strength of wave-induced mixing in a global ocean circulation model. The global distribution of *Bv* averaged over the upper 20 m and the wave-induced mixing depth D_5 show that in boreal summer wave-induced mixing is strong in the Southern Oceans, while in winter it is strong in the North Pacific, the Southern Oceans, and especially in the North Atlantic. The distributions of *Bv* along the dateline in the Pacific and along 30°W in the Atlantic (not shown) appear quite differently. In the Pacific the pattern appears asymmetric in boreal summer, while it is generally symmetric with respect to the equator in the Pacific in boreal winter and in the Atlantic for all seasons. Although the vertical structures are different from each other, there are some similarities between the two oceans, i.e., strong wave-induced mixing appears in respective boreal or austral winters.

[15] Results obtained from a global ocean circulation model coupled to wave-induced mixing indicate an improvement for the simulation of temperature in the upper 100 m. It is thus postulated that wave-induced mixing may play an important role in regulating temperature distribution in the upper ocean. Although the preliminary ocean model calculations indicate the potential for improving global ocean simulations, much more detailed analyses and calibration of the scheme may still be needed.

[16] **Acknowledgments.** This research was supported by the National Key Basic Research Program under contract G1999043809. Comments by the two anonymous reviewers helped to improve this manuscript.

References

Blumberg, A. F., and G. L. Mellor (1987), A description of a three-dimensional coastal ocean circulation model, in *Three-Dimensional Coastal Ocean Models*, *Coastal Estuarine Stud.*, vol. 4, edited by N. Heaps, pp. 1–16, AGU, Washington, D. C.

Craig, P. D., and M. L. Banner (1994), Modeling wave-enhanced turbulence in the ocean surface layer, *J. Phys. Oceanogr.*, *24*, 2546–2559.

Ezer, T. (2000), On the seasonal mixed layer simulated by a basin-scale ocean model and the Mellor-Yamada turbulence scheme, *J. Geophys. Res.*, *105*, 16,843–16,855.

Fang, G., and T. Ichiye (1983), On the vertical structure of tidal currents in a homogeneous sea, *Geophys. J. R. Astron. Soc.*, *73*, 65–82.

Kantha, L. H., and C. A. Clayson (1994), An improved mixed layer model for geophysical applications, *J. Geophys. Res.*, *99*, 25,235–25,266.

Ledwell, J. R., E. T. Montgomery, K. L. Polzin et al. (2000), Evidence for enhanced mixing over rough topography in the abyssal ocean, *Nature*, *403*, 179–182.

Levitus, S. (1982), Climatological atlas of the world ocean, *NOAA Prof. Paper 13*, 173 pp., U.S. Govt. Print. Office, Washington, D. C.

Martin, P. J. (1985), Simulation of the mixed layer at OWS November and Papa with several models, *J. Geophys. Res.*, *90*, 581–597.

Mellor, G. L. (2003), The three-dimensional current and wave equations, *J. Phys. Oceanogr.*, *33*, 1978–1989.

Mellor, G. L., and T. Yamada (1982), Development of a turbulence closure model for geophysical fluid problems, *Rev. Geophys.*, *20*, 851–875.

Polzin, K. L., J. M. Toole, J. R. Ledwell, and R. W. Schmitt (1997), Spatial variability of turbulent mixing in the abyssal ocean, *Science*, *276*, 93–96.

Yuan, Y., Z. Pan, and L. Sun (1991), LAGDF-WAM numerical wave model, *Acta Oceanologica Sinica*, *10*, 483–488.

Yuan, Y., F. Qiao, F. Hua, and Z. Wan (1999), The development of a coastal circulation numerical model: 1. Wave-induced mixing and wave-current interaction, *J. Hydrodyn., Ser. A*, *14*, 1–8.

J. Ma, F. Qiao, C. Xia, Y. Yang, and Y. Yuan, The First Institute of Oceanography, State Oceanic Administration, Qingdao, Shandong 266061, China.

Q. Zheng, Department of Meteorology, 2423 Computer & Space Sciences Building, University of Maryland, College Park, MD 20742-2425, USA. (quanan@atmos.umd.edu)